sustainability

Article

Effective Ti-6Al-4V Powder Recycling in LPBF Additive Manufacturing Considering Powder History

Tejas Koushik [1,2], Haopeng Shen [1,3], Wen Hao Kan [1,3], Mu Gao [1,3], Junlan Yi [4], Chao Ma [4], Samuel Chao Voon Lim [1,3], Louis Ngai Sum Chiu [1,3,*] and Aijun Huang [1,2,3]

1 Monash Centre for Additive Manufacturing, Clayton, VIC 3168, Australia; tejas.maheshkoushik@my.jcu.edu.au (T.K.); haopeng.shen@outlook.com (H.S.); wen.kan@sydney.edu.au (W.H.K.); mu.gao@monash.edu (M.G.); samuel.lim@monash.edu (S.C.V.L.); aijun.huang@monash.edu (A.H.)
2 Mechanical and Aerospace Engineering, Monash University, Clayton, VIC 3168, Australia
3 Materials Science and Engineering, Monash University, Clayton, VIC 3168, Australia
4 Shanghai Aircraft Manufacturing Company, Shanghai 200436, China; yijunlan@comac.cc (J.Y.); machao2@comac.cc (C.M.)
* Correspondence: louis.chiu@monash.edu

Abstract: Laser powder bed fusion (LPBF) is an outstanding additive manufacturing (AM) technology that can enable both complicated geometries and desired mechanical properties in high-value components. However, the process reliability and cost have been the obstacles to the extensive industrial adoptions of LPBF. This work aims to develop a powder recycling procedure to reduce production cost and minimize process uncertainties due to powder degradation. We used a recycle index (R) to reuse Ti-6Al-4V powder through 10 production cycles. Using this recycle index is more reasonable than simply replying on recycle numbers as it incorporates the powder usage history. A recycling procedure with simple virgin powder top-up can effectively mitigate powder degradation and maintain stable powder properties, chemical compositions, and tensile properties. The experimental finding points to a sustainable recycling strategy of Ti alloy powders with minimal material waste and without noticeable detriment to observed mechanical performance through LPBF production cycles.

Keywords: additive manufacturing; powder bed; powder recycling; Ti alloys

check for updates

Citation: Koushik, T.; Shen, H.; Kan, W.H.; Gao, M.; Yi, J.; Ma, C.; Lim, S.C.V.; Chiu, L.N.S.; Huang, A. Effective Ti-6Al-4V Powder Recycling in LPBF Additive Manufacturing Considering Powder History. *Sustainability* **2023**, *15*, 15582. https://doi.org/10.3390/su152115582

Academic Editors: Jan Baeyens and Hosam Saleh

Received: 19 April 2023
Revised: 25 September 2023
Accepted: 28 September 2023
Published: 2 November 2023

1. Introduction

Additive manufacturing (AM) utilizes a layer-by-layer approach to build complex 3D shapes from simple 2D slices. This method provides more freedom to design unique geometries and the ability to integrate multiple assemblies into a single part. There are multiple techniques under the broad umbrella of AM and they are generally categorized by the feedstock forms (powder, wire, liquid, etc.) and the joining techniques (laser sintering, electron beam melting, liquid bonding, UV curing, etc.) [1]. LPBF has been a main AM technology applied in critical sectors because of its ability to produce metallic components with high product quality and mechanical properties [1]. In LPBF processes, only a small portion of the powder is melted and consumed for the final components. The remaining powder is usually retrieved for the next production cycle. This recycling practice is one of the most important measures to reduce the total cost of LPBF. Powder recycling in AM productions can minimize material waste, which has been a paramount feature in modern technologies in the context of sustainability, circular economy, and environmental impact [2].

However, powder degradation occurs with the powder recycling through powder bed AM production cycles, which brings uncertainties in feedstock quality and part integrity. Powder recycling in LPBF production cycles can cause changes in particle sizes, particle morphologies, powder rheology, and chemical composition [3–5]. These changes mainly result from the excessive energy from the laser fusion process. Apart from the desired melting and re-solidification processes, the heating source also forms spatters and agglomerates of partially melted particles [6–8].

In LPBF, the powder re-coater blade moves across from the powder dispenser and coats a uniform layer over the build plate. This process requires a good "spreadability" of the powder to ensure a uniform thin layer of powder. While the spreadability is a qualitative description of the powder, it is usually correlated to the powder flowability which can be quantitatively measured. The powder flowability, a bulk property, depends on its particle size distribution (PSD), morphology, surface chemistry, and moisture level [9]. The powder size and morphology are important considerations in powder metallurgy [10–12]. High densification from high packing density is desired. The powder compaction depends on the powder size distribution and the morphologies. These properties are known to change, and the feedstock variation can affect performance of the final parts produced by LPBF [13–15]. This work selected the Ti-6Al-4V alloy for the reuse study considering it is one of the most important AM alloys for high-value parts widely used in aerospace [16] and biomedical industries [17]. Ti-6Al-4V accounts for up to 60% of all titanium (Ti) alloy production, thanks to its excellent combination of ductility and strength at room and high temperatures [18].

Previous studies have demonstrated this impact on the total LPBF production costs of Ti powders due to the lack of standard powder recycling procedures [19].

Controlling the feedstock quality is critical to the final part quality in LPBF, particularly the microstructure and mechanical properties. Oxygen is an alpha stabilizer and is a known issue in Ti alloy processing as it embrittles the materials and reduces toughness and fatigue properties. The study by Jia [20] showed that increasing oxygen content of Ti-6Al-4V powder during LPBF introduced anisotropy in tensile behavior primarily due to the change of β grain size. Various studies have shown a clear consequence on the microstructure with powder recycling [21]. It was found that increased oxygen content in recycling of Ti-6Al-4V powders was accommodated in the β phase in the LPBF parts. The oxygen pickup and the change of microstructure can reduce fatigue performance and fracture toughness in the LPBF parts built with reused powders.

Other minor elements (e.g., C, N, H) picked up during powder recycling can also affect the powder quality. Silverstein and Eliezer [22] showed that trapped hydrogen during LPBF can lead to formation of TiH that can embrittle the final parts. The source of carbon contamination mainly occurs during powder handling stages and storage. Dissolved carbon in Ti-6Al-4V alloys is known to improve mechanical strength due to precipitation hardening or solid solution strengthening. However, increase in carbon content has been shown to promote grain growth [23]. Presence of nitrogen during LPBF has been shown to increase yield strength and ultimate tensile strength due to a nitrogen solid solution. Further, formation of nano-β phases has been shown to increase with N content during LPBF [24]. However, presence of titanium nitrides can lead to formation of brittle TiN phases that can strengthen the alloy at the cost of reduced ductility.

Nandwana et al. [13] reported a gradual oxygen increase from 0.138 wt.% in the virgin powder to 0.182 wt.% after just five build cycles in electron beam powder bed fusion of Ti-6Al-4V powder. This implies an oxygen pickup rate of 0.011 wt.% per reuse cycle. If the starting feedstock was Ti-6Al-4V Grade 5 powder (max. 0.2% oxygen), it would exceed the qualification range after about 6 times of recycling. Another study of electron beam powder bed fusion of Ti-6Al-4V also reported a very different oxygen pickup rate at about 0.005% increase per reuse cycle from 0.08 wt.% in the virgin powder to 0.19 wt.% after 21 times of recycling [14]. To maintain the material qualification for Ti-6Al-4V ELI powder (Grade23, max. 0.13 wt.% oxygen), this production condition would allow recycling up to about 10 times. The actual experiment results showed that the powder went above 0.13 wt.% after only 6 reuse cycles. This indicated that relying on the number of reuse cycles to control the powder quality is not reliable. Quintana et al. [4] performed a study on recycling Ti-6Al-4V powders in LPBF production cycles, which also showed a progressive increase at about

0.000645% per cycle in oxygen pickup, from 0.09 wt.% in the virgin powder to 0.11 wt.% after 31 reuse cycles. To maintain the material qualification for Ti-6Al-4V ELI powder, their LPBF production setup would allow recycling up to about 62 times. Another similar study on Ti-6Al-4V powder recycling with a different LPBF system showed a similar trend but different oxygen pickup rate [25]. Shalnova et al. [26] studied the effect of powder recycling in laser direct energy deposition (DED). They found that the argon protection could effectively control powder oxidation. The parts built with initial powder (0.079% oxygen) and recycled powder (0.099% oxygen) showed negligible microstructure difference. The micro hardness increased slightly in the parts built with recycled powder. The strength fluctuated without showing an obvious trend with more recycling. They concluded that no tangible changes to mechanical properties were detected in the annealed DED samples with an increase of used Ti-6Al-4V powder content up to 50% in the build. Different from Shalnova et al. [26], Yang et al. [27] conducted a recycle study in a reactive atmosphere with various oxygen level. They found that parts built with recycled powder had coarse α lamellar thickness and higher β phase content than those built with fresh powder. They found that the tensile strength increased slightly with more oxygen pickup in the final parts, which agrees with the study by Shalnova et al. [26]. Derimow and Harabe [28] showed that oxidation rates Ti-6AL-4V powder differed during LPBF and electron beam PBF irrespective of the powder reuse strategy. This was attributed to the higher temperature achieved during build production. Formation of surface oxide layer on powder particles can lead to a lack of fusion during electron beam PBF, which will cause a reduction in part strength [15]. Lastly, residual oxygen content present in the powder handling systems could also contribute to an increase in oxygen content.

These recycling studies all pointed to a fact that the number of reuse cycles cannot be used as a reliable index to control the feedstock quality regarding oxygen pickup. To control the quality of the reused powder, the process history of each build cycle must be considered.

Build number or recycle number has been the common metric to evaluate the powder degradation during powder recycling in LPBF productions. However, the actual powder degradation depends on the process conditions and environment in LPPBF system, especially the energy input and solidification volume, which generates spatters as the main source of contaminants [21,29]. This work aims to develop and evaluate build volume ratio (BV ratio) and recycle index (R index) to consider the solidification percentage and powder usage history through LPBF builds. The findings can contribute to more reliable powder recycling to reduce material cost and improve the sustainability of LPBF productions.

2. Methods

2.1. System and Powder

This work used an industrial LPBF system EOS M290 (EOS GmbH, Krailling, Germany), which is equipped with a 400 W Yb-fiber laser and a beam focus of 100 µm. All the LPBF productions used high-purity argon gas (purity > 99.997%) to ensure minimal oxidation. All components and test samples manufactured in this study used a layer thickness of 30 µm. The process parameters were optimized parameters developed for Ti-6Al-4V powders to obtain high-density parts (relative density > 99.9%).

Commercially available plasma atomized Ti-6Al-4V Grade 23 powder (supplied by AP&C Inc., Montreal, QC, Canada) was used in the LPBF builds. This study refers to the as-received powder from the manufacturer as the virgin powder (Composition specification shown in Table 1). The virgin powder had a particle size range between 15 µm and 45 µm. The chemical composition of the reused powders was investigated throughout the recycle builds.

Table 1. Chemical composition of the Ti-6Al-4V Grade 23 virgin powder.

	Ti	Al	V	Fe	O	C	N	H
wt.%	Balance	6.27	3.94	0.20	0.107	0.019	0.009	0.002

2.2. Characterization and Testing

The chemical compositions were analyzed by a commercial lab (Luvak Inc., Boylston, MA, USA). The elements were measured according to the methods specified in international standards: inert gas fusion for oxygen and nitrogen (ASTM E1409) [30], combustion infrared detection for carbon (ASTM E1941) [31], inert gas fusion for hydrogen (ASTM E1447) [32], and direct current plasma emission spectroscopy for all other elements (ASTM E 2371) [33].

The physical properties analyzed for the reused powders included: (1) presence of contaminants; (2) particle size and shape; (3) apparent density; (4) flowability; and (5) moisture. The particle size distribution of the powders was determined using a laser diffraction instrument (Mastersizer 2000, Malvern, UK) according to the method as specified in ASTM E2651-19 [34]. The particle size analysis has a repeatability of ±0.5 µm.

The powder flowability was determined using the Hall flow test. It measures the time taken for exactly 50 g of powder to flow through an orifice, reported as seconds/50 g. Free flowing powders are defined as powders that can pass the Hall flow test and non-free flowing powders refers to powders that are unable to pass this test. This work used the Carney flow test to measure the flowability of non-free flowing powders in the Hall flow test. The procedures for the Hall flow test and the Carney flow test were conducted according to ASTM B855 [35] and ASTM B964-16 [36] standards, respectively. The apparent density of the powders was also measured to quantitatively compare the packing efficiency of the reused powders. In the SLM process, the packaging efficiency of the powders between the individual layers can affect the laser absorption, defect formation, and surface finish of the final parts. The measurement of apparent density was carried out for free-flowing powders according to ASTM B417 standard [37] and non-free flowing powders according to ASTM B212 standard [38].

The Hausner ratio indicates the compaction of the powder. It is calculated by dividing the apparent density and tap density. Tap density along with apparent density allows us to quantify the interparticle friction which is an essential powder characteristic affecting its ability to produce uniform layers during powder spreading [39]. The tap density was measured by feeding powder into an empty cylinder. The cylinder is then tapped on a fixed platform until there is no visible change in the height of the powder. The powder was then weighed using an analytical balance, the tap density was determined by dividing the mass with measured volume of the powder [40]. The Hausner ratio is calculated by dividing the apparent density and tap density.

The porosity and microstructure of samples built with reused powders was measured using image analysis of polished section. The samples were ground with SiC grinding papers gradually from 300 up to 4000 grit and polished with 0.25 µm OP-S colloidal silica solution. The images were captured using an optical microscopy (Olympus PMG-3) and analyzed using ImageJ software (V1.53k). To observe the microstructure, polished samples were immersed in Kroll's reagent for 30 s.

Cylindrical samples were built to investigate the effect of powder recycling on mechanical properties. The cylindrical bars for tensile specimens were heat treated at 800 °C for 6 h in a vacuum furnace after the LPBF builds. This heat treatment is known to give a good balance of strength and ductility to the final parts [41]. First, it decomposes the brittle α phase to $\alpha+\beta$ phases. It also relieves the residual stresses from the laser melting and re-solidification process. Both effects improve the ductility. After the heat treatment, the cylindrical bars were machined into tensile specimens and tested according to the ASTM E8/E8M standard [42]. The diameter and length of the gauge section were 48 mm and 6 mm, respectively. The tensile samples were machined with a fine finishing to the final diameter with a ±0.01 mm precision. The measured diameters were used during tensile testing.

2.3. Quantifying Powder Recycling

This study adopted a powder refreshing method by mixing virgin powder with reused powder throughout the LPBF builds to control the powder quality. The flow chart in Figure 1 describes the procedures for the powder feedstock used in each build.

diameter with a ±0.01 mm precision. The measured diameters were used during tensile testing.

2.3. Quantifying Powder Recycling

This study adopted a powder refreshing method by mixing virgin powder with reused powder throughout the LPBF builds to control the powder quality. The flow chart in Figure 1 describes the procedures for the powder feedstock used in each build.

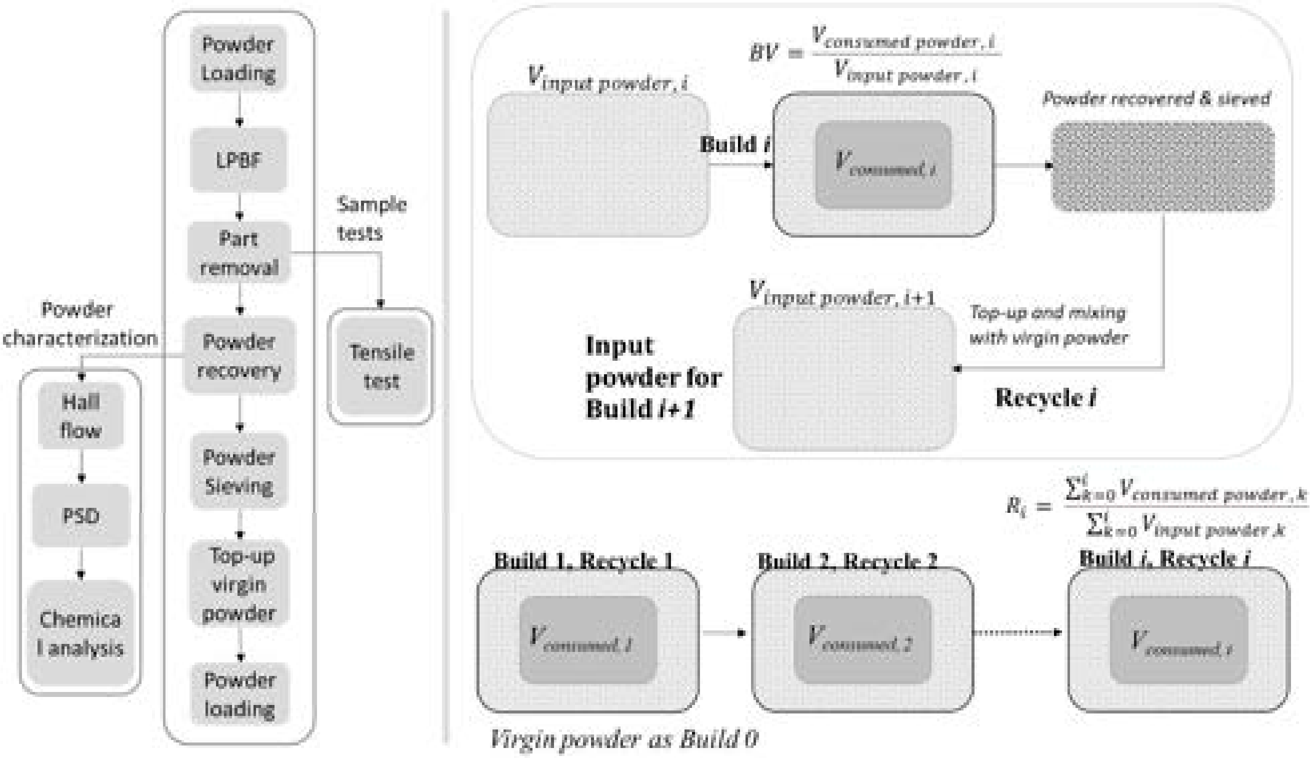

Figure 1. Experiment procedures and schematic for the BV ration and R index.

To quantify the powder recycling, this work introduced a build volume ratio (BV) by dividing the total volume of the components and the total volume of the powder dispensed into the build chamber for the printing job (Equation (1)). To capture the effect of multiple builds and the mixing of virgin and used powder, a recycle index (R) is defined as a ratio of volume of powder consumed to the input volume of powder. The recycle index for build *n* is shown in Equation (2).

$$\text{BV ratio} = \frac{V_{consumed\ powder}}{V_{input\ powder}} \quad (1)$$

$$\text{R index} = \frac{\sum_{k=0}^{i} V_{consumed\ powder,k}}{\sum_{k=0}^{i} V_{input\ powder,k}} \quad (2)$$

where $V_{consumed}$ is the powder volume used in a specific build. This powder consumed in the build is about the same mass as the laser solidified parts and the spatters sieved out in the recovered powder. Powder was carefully retrieved the sieved to minimize powder loss. The R index considers the total powder consumed from build 1 to build i. For example, if 50% of 1 kg powder is used in build 1, then for build 2 feedstock, the R index is 0.5 if no virgin powder is topped up; or the R index is 0.33 if another 0.5 kg powder is added to make a 1 kg input powder for build 2.

The significance of the R index is that it is compatible with different types of recycling studies. Currently, two different recycling approaches exist in the literature: the single-batch and the top-up approaches. At first glance, they are not comparable. However, both approaches can be made comparable via the R index, if the volumes of the input powder and solidified material for each build in the series are known. This allows for the determination of equivalence across different approaches as well as builds of different sizes or on different machines.

The key assumption made in establishing the R index is that the effect of recycling correlates linearly with the amount of solid material built and there are no interaction effects. The reason for this set of assumptions is based on the physical setup of the SLM process. During the laser melting process, only the powder in a small region near the scan approaches can be made comparable via the R index, if the volumes of the input powder and solidified material for each build in the series are known. This allows for the determination of equivalence across different approaches as well as builds of different sizes or on different machines.

The key assumption made in establishing the R index is that the effect of recycling correlates linearly with the amount of solid material built and there are no interaction effects. The reason for this set of assumptions is based on the physical setup of the SLM process. During the laser melting process, only the powder in a small region near the scan track will experience a change in temperature that can cause degradation. This area will be proportional to the scan track length, which in turn is proportional to the scan area. In addition, only the powder dispensed into the build chamber is considered as the powder that remains undispersed was not affected by factors detrimental to its quality. Therefore, this single index represents the combined effects of repeated laser exposure, heating and cooling cycles, accumulation of sputter, agglomeration, sintering, and chemical change of powder as it is being repeatedly used.

The R index allows one to quantify the history of the powder batch based on the extent of previous use which incorporated the volume of the part built. This allows the quantification of the extent of recycling to a greater degree of accuracy. Since the builds are not the same, simply counting the number of times that the powder was reused is insufficient to describe the extent of recycling, which is the conventional method. Moreover, the addition of virgin powder is an additional variable that the conventional method cannot capture. In the present study, the BV ratios for each build in the sequence within this study and R indices of the input powder for these builds are as indicated in Figure 2.

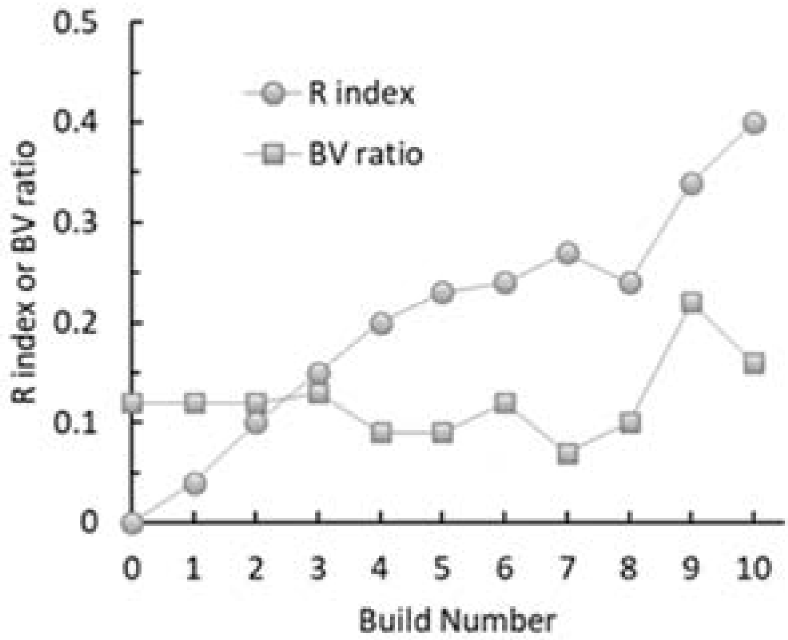

Figure 2. Variation of the BV ratio and R index across the recycle builds (build 0 represents the virgin powder).

To extract the most information out of the recycling build, the build program is separated into three separate regimes. For build 0 (virgin powder) to build 3 (3rd reuse cycle build), the BV is constant. In builds 4 to 7, a variety of BVs are utilized to confirm the assumption of the linear relationship between powder degradation and the amount of solid built. This is particularly important when applied to an industrial setting in pursuit of ever greater customization which is a major advantage offered by additive manufacturing. Beginning from build 8, previously reused powder of various extents of recycling was used in the top-up process to give an indication of the overall applicability of the present approach.

The R index was used to track the extent of recycling in the present study. The state of the powder particles as well as the resultant microstructure and tensile properties at an R index of 0.00, 0.04, 0.15, 0.24, and 0.40 were characterized to understand the effect of powder reuse. Note that the R index corresponds to the state of the powder at the start of the build, since the R index would increase at the end of the build due to the solid material built during the build. These R indices correspond to the use of virgin powder and powder at the 1st, 3rd, 6th, and 10th reuse cycle (topped up as necessary) in the respective builds.

The R index was used to track the extent of recycling in the present study. The state of the powder particles as well as the resultant microstructure and tensile properties at an R index of 0.00, 0.04, 0.15, 0.24, and 0.40 were characterized to understand the effect of powder reuse. Note that the R index corresponds to the state of the powder at the start of the build, since the R index would increase at the end of the build due to the solid material built during the build. These R indices correspond to the use of virgin powder and powder at the 1st, 3rd, 6th, and 10th reuse cycle (topped up as necessary) in the respective builds.

3. Results and Discussion

3.1. Quantifying Powder Recycling

3.1.1. Morphology

The SEM images of the powder recovered from build 10 shown in Figure 3b showed no loss in sphericity, but the number of observed satellites gradually increased as compared to the virgin powder in Figure 3a. This is consistent with previous studies that have reported a reduction of sphericity only after 30 build cycles [4]. The sieved-out debris contained the unwanted agglomerates and sintered powder clusters that were expected from the SLM process. This demonstrated that sieving using a 63 µm sieve effectively maintained powder morphology quality in the reused powder.

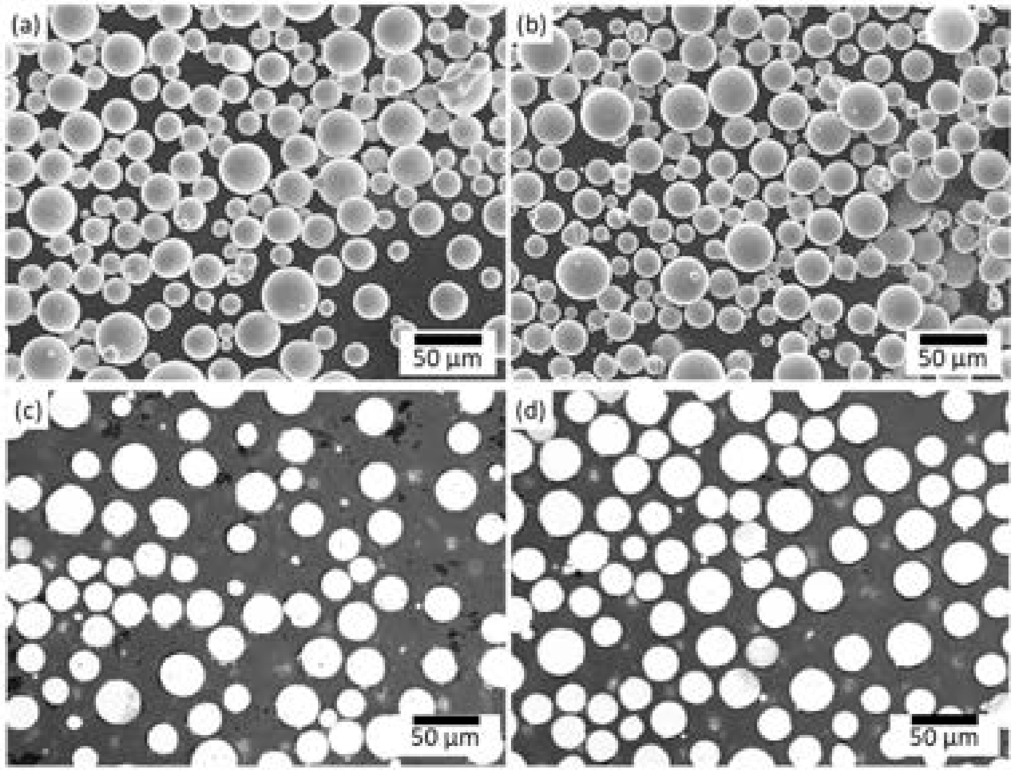

Figure 3. The virgin powder and the recycled powder (after sieving and refreshing of virgin powder) showed very similar morphology in SEM images of (**a**) virgin powder before build 1, (**b**) recycled powder at build 10, and in optical images showing the corresponding the polished cross sections of the (**c**) virgin powder and (**d**) the recycled powder.

3.1.2. Particle Size Distribution

Particle size distribution study using laser diffraction on the powder samples, shown in Figure 4, revealed that the average particle size of the D50 remains at 31 µm ± 2 µm over the entire study. A similar trend could be observed in the case of the D10 and D90, having an average value of 21 µm (±2 µm) and 50 µm (±1 µm), respectively. The present results compare favorably with the existing literature. Quintana et al. [4] reported a steady D10 and D50 value and a slightly decreasing D90 with increased recycling. The slight reduction in D90 was attributed to the sieving step included prior to every build; eliminating the larger particles with satellites and agglomerates which had accumulated because of repeated laser exposure. In contrast, Alamos et al. [43] reported that while there is no change in the D50 and D90 values, the D10 value increased slightly between the virgin powder and the 1st recycle build and then remained constant over subsequent builds.

powder and the 1st recycle build and then remained constant over subsequent builds.

The constant D90 result showed that the sieving step is effective at removing the larger agglomerates and powder clusters produced during the SLM process, while the D10 results show that the smaller particles are not preferentially consumed or otherwise removed during the handling process as summarized by Alamos et al. [43]. Overall, our recycling process has demonstrated its ability to control the various factors and maintain the desired PSD.

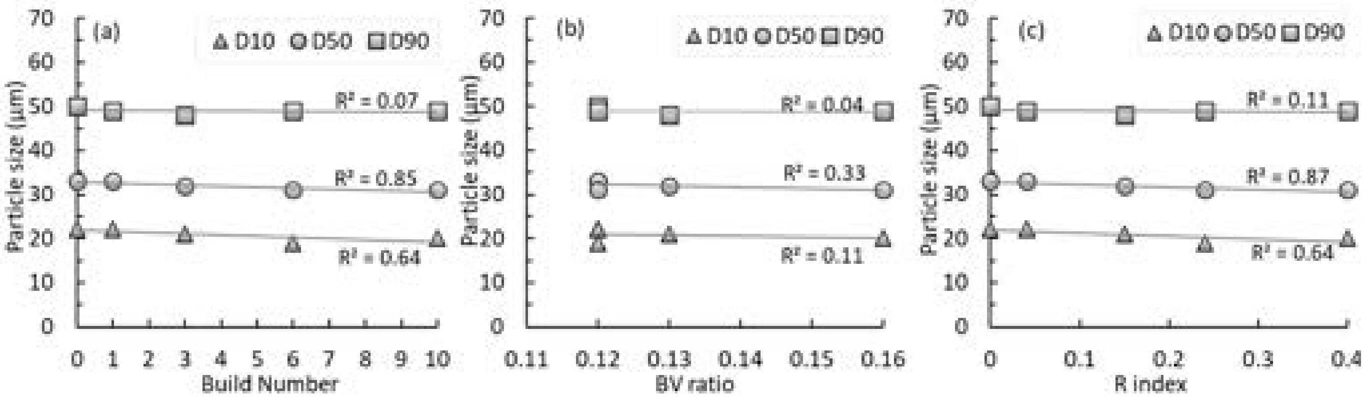

Figure 4. PSD variation with increasing extent of powder recycling represented by (**a**) build number, (**b**) BV ratio, and (**c**) R index. The solid lines represent the linear regression.

The constant D90 result showed that the sieving step is effective at removing the larger agglomerates and powder clusters produced during the SLM process, while the D10 results show that the smaller particles are not preferentially consumed or otherwise removed during the handling process as summarized by Alamos et al. [43]. Overall, our recycling process has demonstrated its ability to control the various factors and maintain the desired PSD.

3.1.3. Flowability

The Hall test performed on the reused powder (Figure 5a) showed an improved flowability after the 1st recycling step and remained relatively steady for all subsequent builds. Similarly, a very slow decline in the Hausner ratio was observed (Figure 5b). This observation is consistent with the reused powder retaining its sphericity through the number of build cycles [44]. The consistency of the flowability characteristics is indicative of the inter-particle friction being constant through the recycling process and that loss of sphericity or contamination [45] had not occurred.

3.1.3. Flowability

The Hall test performed on the reused powder (Figure 5a) showed an improved flowability after the 1st recycling step and remained relatively steady for all subsequent builds. Similarly, a very slow decline in the Hausner ratio was observed (Figure 5b). This observation is consistent with the reused powder retaining its sphericity through the number of build cycles [44]. The consistency of the flowability characteristics is indicative of the inter-particle friction being constant through the recycling process and that loss of sphericity or contamination [45] had not occurred.

It should be mentioned that the virgin powder (at build 0), although it had a size similar to the recycled powder, showed worse flowability. The powder did not pass the Hall flow test, therefore there is no Hall flow rate at build 0 in Figure 5d. A possible reason is that the power of a size at 31 µm (D50) is in the transition zone from non-flowing powder to free-flowing powder, as reported in the work by Shen et al. [46]. They reported that the flowability of Ti alloy powder of around 30 µm can be improved significantly as the heat in a build cycle reduces the mois-

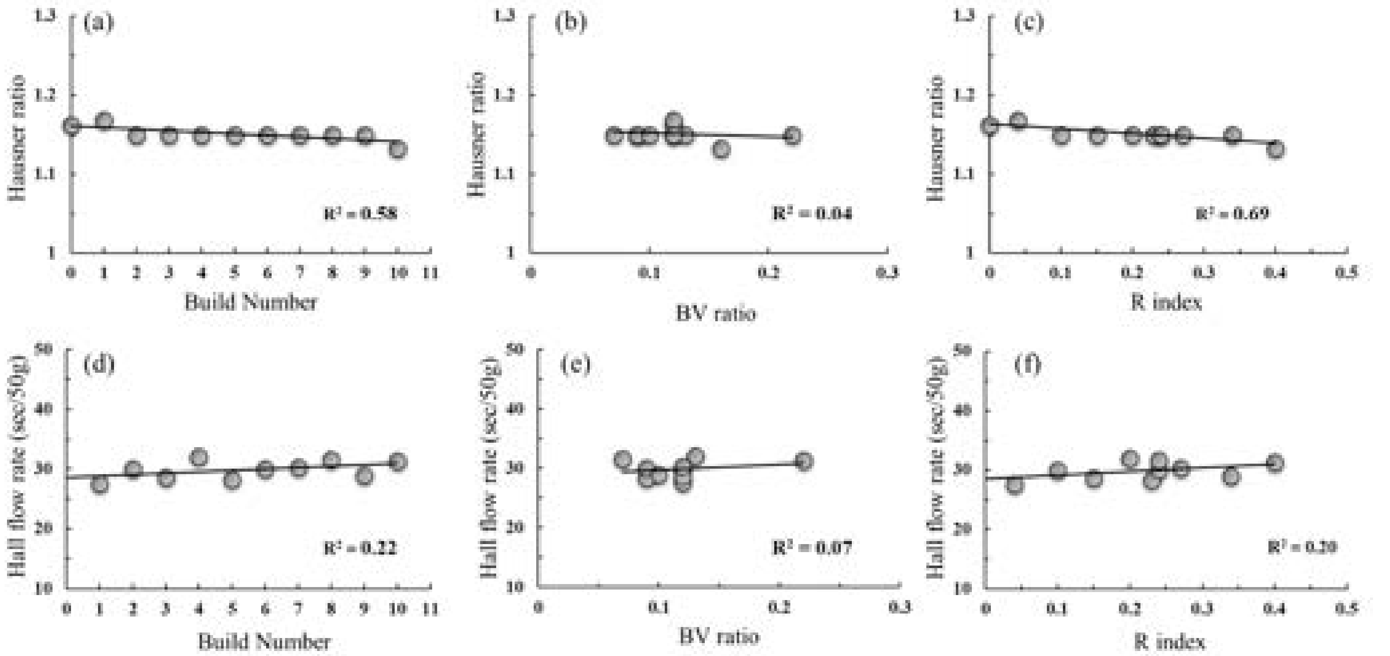

Figure 5. (**a**–**c**) Powder packing (Hausner ratio) and (**d**–**f**) powder flowability (Hall flow) showed no obvious trend with increasing powder recycling represented by build number, BV ratio, or R index. Solid lines show the linear fitting. The coefficient of determination R2 indicates the goodness of the linear fitting.

The unchanging surface morphology, PSD, and flowability characteristics as the powder is recycled in the various builds indicate that the spreadability of the powder is maintained. Coupled with the fact that the recycling was using unequal build volumes, one can reach the conclusion that as long as the R index is below 0.40, the recoat charac-

It should be mentioned that the virgin powder (at build 0), although it had a size similar to the recycled powder, showed worse flowability. The powder did not pass the Hall flow test, therefore there is no Hall flow rate at build 0 in Figure 5d. A possible reason is that the power of a size at 31 µm (D50) is in the transition zone from non-flowing powder to free-flowing powder, as reported in the work by Shen et al. [46]. They reported that the flowability of Ti alloy powder of around 30 µm can be very sensitive to moisture level. The flowability can be improved significantly as the heat in a build cycle reduces the moisture level [46].

The unchanging surface morphology, PSD, and flowability characteristics as the powder is recycled in the various builds indicate that the spreadability of the powder is maintained. Coupled with the fact that the recycling was using unequal build volumes, one can reach the conclusion that as long as the R index is below 0.40, the recoat characteristics are preserved.

3.1.4. Powder Chemistry

The powder chemistries of reused powder shown in Figure 6 appear to be very similar except for a slight increase in oxygen content. The chemical composition of the reused powder remained within standard specifications for Ti-6Al-4V grade 23. The source of the increased oxygen content can be attributed to spatter inclusion in the powder batch during laser exposure [4]. Nandwana et al. [13] showed that source of oxygen was more from the sudden absence of vacuum in the powder recycling system of electron beam melting machines, this was further illustrated in multiple studies [21]. Harkin et al. [47], utilizing a top-up recycling strategy for laser powder bed fusion, indicated that oxygen content reached the maximum acceptable value of 0.13% at the 8th cycle of powder reuse. In our study (as shown in Figure 6), the increase in oxygen reported between each build is small due to the recycling strategy that was employed here. Adding virgin powder to every build cycle progressively dilutes the oxygen content and allows the powder batch to remain within specifications for Ti-6Al-4V grade 23 powder. Furthermore, the correlation of R index and oxygen content (Figure 6c), were found to be higher compared to build number (Figure 6a), which indicates that the R index could be a better indicator of oxygen content compared to the conventionally used build number. In other words, the powder oxygen content "remembers" the powder usage history.

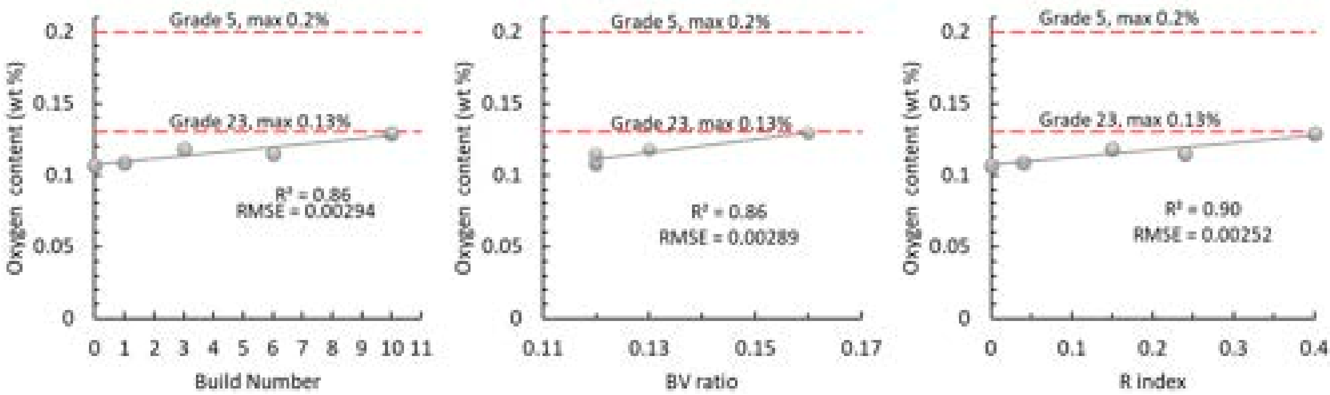

(**a**) (**b**) (**c**)

Figure 6. Variation of oxygen content as a function of (**a**) build number, (**b**) BV ratio, and (**c**) R index. Dashed lines at 0.13% and 0.2% show the maximum allowable oxygen content for Grade 23 and Grade 5 Ti-6Al-4V powders, respectively. Solid lines show the linear fitting. R^2 and root mean squared errors (RMSE) values are included to show the goodness of the linear fitting.

Figure 6. Variation of oxygen content as a function of (**a**) build number, (**b**) BV ratio, and (**c**) R index. Dashed lines at 0.13% and 0.2% show the maximum allowable oxygen content for Grade 23 and Grade 5 Ti-6Al-4V powders, respectively. Solid lines show the linear fitting. R^2 and root mean squared errors (RMSE) values are included to show the goodness of the linear fitting.

3.2. Build Material Characterisation

3.2.1. Density and Microstructure

The built material exhibited very high density across all the recycle builds. A material density of between 99.51% to 99.92% was achieved in all builds in the present study. Figure 7 shows a typical cross section of the built material.

Build Number BV ratio R index

(a) (b) (c)

Figure 6. Variation of oxygen content as a function of (**a**) build number, (**b**) BV ratio, and (**c**) R index. Dashed lines at 0.13% and 0.2% show the maximum allowable oxygen content for Grade 23 and Grade 5 Ti-6Al-4V powders, respectively. Solid lines show the linear fitting. R^2 and root mean squared errors (RMSE) values are included to show the goodness of the linear fitting.

3.2. *Build Material Characterisation*

3.2.1. Density and Microstructure

The built material exhibited very high density across all the recycle builds. A material density of between 99.51% to 99.92% was achieved in all builds in the present study. Figure 7 shows a typical cross section of the built material.

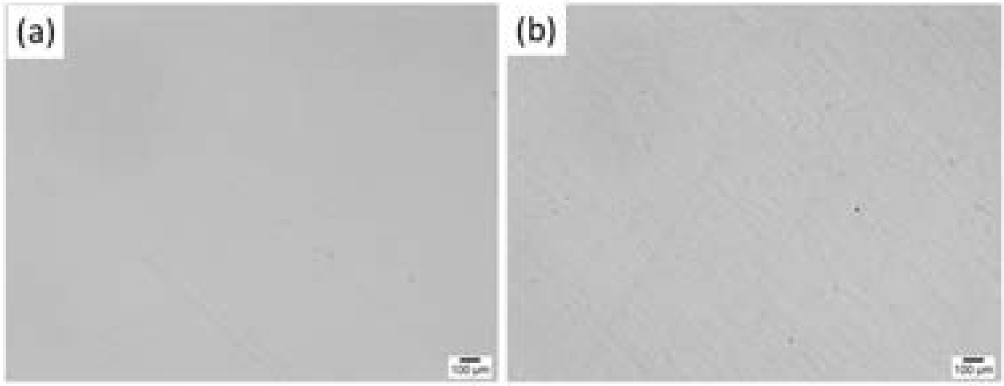

Figure 7. (**a**,**b**) Representative cross-sectional images taken from two different regions of the as-built samples (recycle 10 build) showing very little visible porosities. The measured relative density was above 99.9% for all samples.

Microstructure characterization of the as-built components after heat treatment at 800 °C for 6 h revealed an $\alpha + \beta$ type microstructure as shown in Figure 8. The white lamellae represent the α phase and the dark regions represent the β phase. The microstructure of the material built using reused powder is typical of that of Ti-6Al-4V alloy. The high cooling rates of L-PBF lead to the initial formation of martensitic structures. The heat treatment as suggested by Cao et al. [41] was implemented in this study to ensure the maximum conversion of martensite into $\alpha + \beta$ phases, leading to the formation of a Widmanstätten pattern. This conversion of the martensitic structure results in a drop in ultimate tensile strength (UTS) and yield strength (YS) while improving elongation (i.e., >12% elongation) of the resulting material, as will be shown below in the next section in Table 2. The microstructure observed resembles the microstructure usually reported in Ti-6Al-4V alloys processed using electron beam-assisted melting [15].

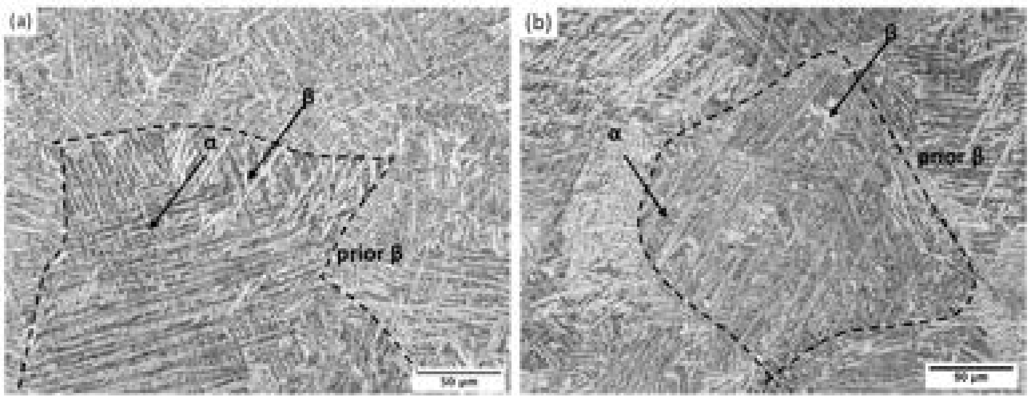

Figure 8. The heat-treated samples built with different levels of recycling show similar microstructure, showing visible prior β boundaries, colonies of acicular α phases, and transformed β phases. (**a**) recycle build 2 and (**b**) recycle build 6.

The highly consistent microstructure in Figure 8 was also mirrored by the fracture surfaces where identical features were exhibited (Figure 9).

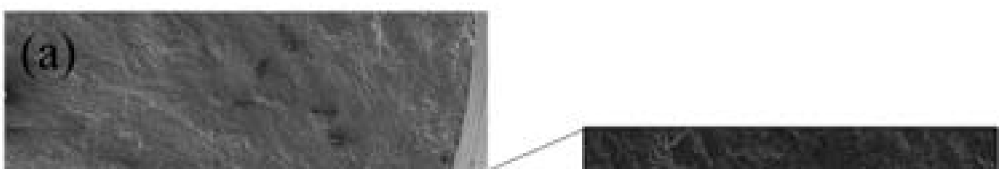

Figure 8. The heat-treated samples built with different levels of recycling show similar microstructure, showing visible prior β boundaries, colonies of acicular α phases, and transformed β phases. (**a**) recycle build 2 and (**b**) recycle build 6.

The highly consistent microstructure in Figure 8 was also mirrored by the fracture surfaces where identical features were exhibited (Figure 9).

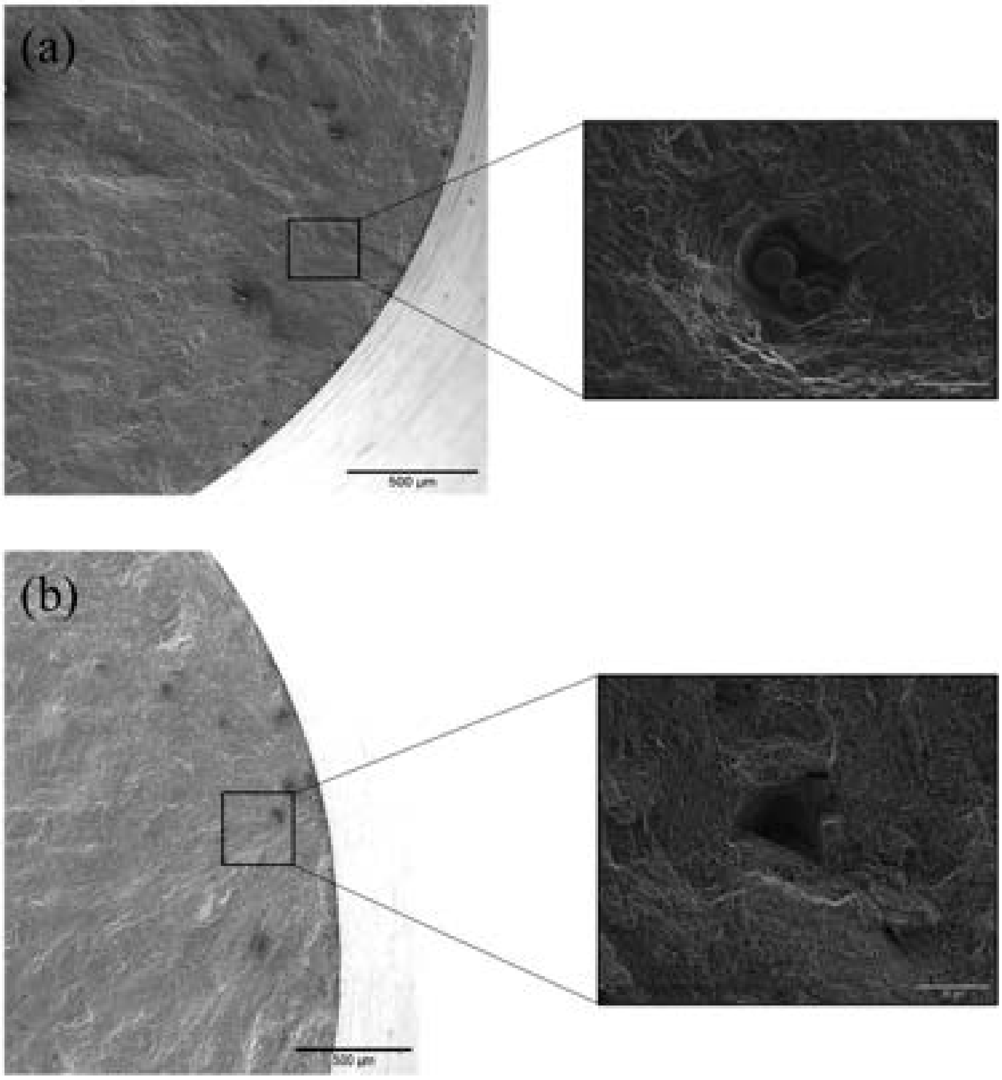

Figure 9. Fracture surface of sample from recycle build 1 (**a**) and recycle build 6 (**b**).
Figure 9. Fracture surface of sample from recycle build 1 (**a**) and recycle build 6 (**b**).

3.2.2. Tensile Performance

The tensile results from this study are shown in Table 2. The changes of the tensile properties are minor, and the properties conform with the AMS 4928 (Committee 1957) mechanical properties minimum standard, i.e., 896–930 MPa tensile strength, 820–860 MPa yield strength, 8–10% elongation, and a 10–25% area reduction. The mechanical properties from work on reused powder builds in the literature are also shown and compared in Table 2. Most of the existing literature utilized the single batch approach recycling with sieving, where no powder is added during recycling. This method would be considered the more adverse condition for the reused powder than the top-up method used in the present study using virgin powder to refresh the feedstock.

The present mechanical results are consistent with that reported in the literature. Very minor increases in YS and UTS with increasing extent of recycling have been attributed to oxide inclusions during powder recycling [20] and/or pick-up during the building process [14,48]. However, others have reported no correlation between oxygen pick-up and the small increase in the YS and UTS [4]. On the other hand, the oxygen content of the built components in the present study was not a good indicator of the mechanical properties of heat treated components, which is in contrast with Tang et al.'s [14] finding.

Table 2. Comparison of tensile results of the AM build between present study and literature.

	Process Condition	Recycle Method	Recycle Times/BV Ratio/ R Index	Powder/ (Part) Oxygen Content (%)	Mechanical Properties			
					YS (MPa)	UTS (MPa)	E (ε)	R.A (%)
Present study	LPBF and heat treated at 800 °C 6 h	Sieving and refreshing	0/0.12/0	0.107	948 ± 8	1034 ± 5	16.0 ± 2.0	36 ± 6
			1/0.12/0.04	0.109	946 ± 14	1035 ± 6	17.0 ± 1.0	38 ± 2
			3/0.13/0.15	0.118	929 ± 23	1035 ± 6	17.0 ± 1.0	38 ± 3
			6/0.12/0.24	0.115	939 ± 27	1033 ± 17	16.0 ± 1.4	37 ± 5
			10/0.16/0.40	0.129	930 ± 28	1033 ± 17	14.5 ± 1.0	40 ± 5
[43]	LPBF and heat treated at 650 °C 3 h then 800 °C 2 h	Sieving only	0	(0.125)	933 ± 5	1030 ± 4	15.7 ± 0.5	56 ± 2
			1	(0.110)	938 ± 9	1027 ± 5	17.3 ± 0.4	59 ± 1
			4	(0.120)	947 ± 6	1034 ± 3	15.3 ± 0.3	54 ± 1
			8	(0.125)	958 ± 7	1043 ± 2	15.3 ± 0.3	51 ± 1
[25]	LPBF and heat treated in vacuum	Sieving only	1	0.090	839	1012	7	14
			12	0.103	934	1052	12	30
			18	0.119	921	1056	17	42
			24	0.122	918	1051	7	12
			31	0.119	897	1041	10	18
			38	0.121	989	1095	17	47
[4]	LPBF and HIP at 920 °C 102 MPa 2 h	Sieving only	1	0.11	879 ± 7.6	984 ± 0.6	14 ± 0.6	44 ± 0.6
			4	0.13	871 ± 6.0	988 ± 1.0	15 ± 0.6	45 ± 1.2
			17	0.12	893 ± 3.1	1001 ± 0.6	15 ± 0.0	47 ± 0.0
			31	0.11	881 ± 3.6	1003 ± 1.2	15 ± 0.6	44 ± 0.6
[49]	LPBF and heat treated at 704 °C 1 h	Sieving only	0	0.10	992	1090	14.0	-
			15	0.12	978	1073	14.5	-
[14]	EBM, preheat to 730 °C	Sieving only	0	0.08	834 ± 10.0	920 ± 10.0	16 ± 0.3	54 ± 3.0
			2	0.097	870 ± 8.0	970 ± 10.0	15 ± 0.3	46 ± 3.0
			6	0.14	822 ± 25.0	910 ± 20.0	14 ± 1.0	53 ± 4.0
			11	0.17	892 ± 4.5	987 ± 3.5	18 ± 0.8	50 ± 1.0
			16	0.18	940 ± 3.6	1028 ± 4.1	15 ± 1.8	42 ± 4.1
			21	0.19	960 ± 30.0	1039 ± 2.7	16 ± 0.9	-

As shown in Table 2, this work obtained very consistent tensile properties. The variation of average yield strength is only −22% (−19 MPa) from the virgin powder build. The results from the work by Park et al. [25] and Tang et al. [14] showed a significant increase of yield strength +150 MPa (+18%) and +126 MPa (+15%). The increase can be attributed to the effect of oxygen pickup in the powder which strengthens the material. However, the fracture toughness and fatigue properties may be reduced.

Taking a close look at the yield strength in this work, it can be found in Figure 10 that the yield strength decreased with increasing extent of powder recycle. Comparing build number, BV ratio, R index, the yield strength showed the best correlation with BV ratio. This implies that during the LPBF production, a larger volume resulted in a noticeable decrease in the yield strength. A possible reason is the spatters generated during laser melting. These spatters are usually larger than the feedstock powder particles. The larger size can cause lack of fusion issues, which may introduce more defects in the parts, which reduces the yield strength. However, the cross sections did not show a clear change of porosity in the parts. More careful inspections using X-ray micro-CT can help to improve understanding.

Sustainability **2023**, *15*, x FOR PEER REVIEW 13 of 18

to the effect of oxygen pickup in the powder which strengthens the material. However, the fracture toughness and fatigue properties may be reduced.

melting. These spatters are usually larger than the feedstock powder particles. The larger size can cause lack of fusion issues, which may introduce more defects in the parts, which

porosity in the parts. More careful inspections using X-ray micro-CT can help to improve understanding.

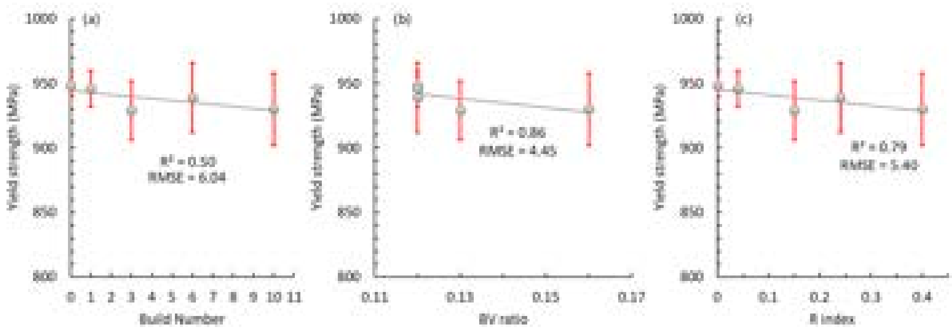

Figure 10. Observed variation in material yield strength as a function of (**a**) build number, (**b**) BV ratio, and (**c**) R index. The solid lines represent the trends associated with each plot. R^2 and root mean squared errors (RMSE) values are included to show the goodness of linear fitting.

3.3. Assessment of Powder Processing Methodology

The key issue in the present work is to establish whether the proposed methodology can ensure that the used powder can be returned to a state that is comparable to that of virgin powder to ensure consistent powder properties and material performance. Previously, in Section 3.1, the quality of the processed powder was evaluated and it was demonstrated that the recycled powder met the same characteristic and performance criteria as the virgin powder. In addition, Section 3.2 established that the performance of the built material was indistinguishable from that built using the virgin powder. In this section, heat-affected powder collected near the gas outlet and the oversized powder col-

3.3. Assessment of Powder Processing Methodology

The key issue in the present work is to establish whether the proposed methodology can ensure that the used powder can be returned to a state that is comparable to that of virgin powder to ensure consistent powder properties and material performance. Previously, in Section 3.1, the quality of the processed powder was evaluated and it was demonstrated that the recycled powder met the same characteristic and performance criteria as the virgin powder. In addition, Section 3.2 established that the performance of the built material was indistinguishable from that built using the virgin powder. In this section, heat-affected powder collected near the gas outlet and the oversized powder collected in the sieving process were analyzed to gain a better understanding of the mechanism behind the effectiveness of the proposed processing methodology.

In the EOS M290 LPBF machine (EOS GmbH, Krailling, Germany) used in this study, the protective argon gas forms a shielding gas flow over the powder bed to remove fumes and spatters during the LPBF process. The heat-affected powder samples were collected from the build platform near the gas outlet. This sample was composed of unused powder and the heated-affected particles that were redistributed by the gas flow. The sieved-out spatter samples were the oversized particles sieved out using a 53 µm mesh. These particles were formed from partial sintering of powder particles into clusters due to the laser energy in the LPBF process as well as any larger process-affected material. The oversized particles sieved out during the powder recycling have a much higher oxygen and nitrogen content compared to the virgin powder (Figure 11), which proved that the sieving process can remove powder that had its chemical composition altered by the laser scan process.

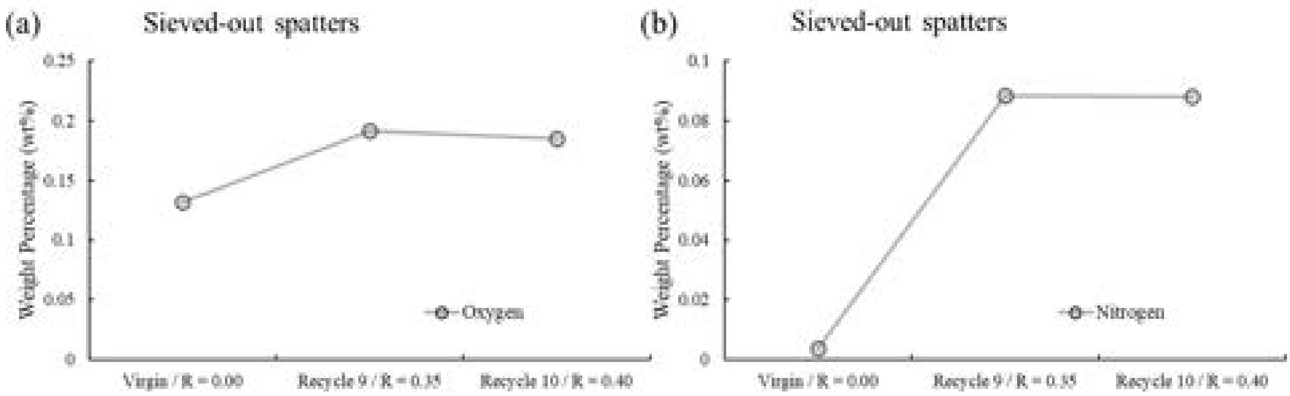

Figure 11. Chemical composition of oversize particles compared with the virgin powder: (**a**) oxygen content, (**b**) nitrogen content.

However, it is impossible to measure the total amount of process-affected material and sintered clusters generated over the course of a build that can degrade the powder batch. By assessing the PSD of the heat-affected particles and sieved-out spatters (Figure 12), as well as the PSD (Figure 5) and chemical composition (Figure 6) of the sieved recycled powder, the effectiveness of the recycling process can be inferred. The PSD of the heat-affected particles encompassed a large range, substantially larger than that of the reference virgin powder. This is consistent with its expected composition of unused powder and process-affected material (which is supported by their trace chemical composition, Figure 13). The sieved-out particle samples had a PSD exclusively above that of the reference virgin powder, i.e., the D10 of the oversized powder was higher than the D50 and close to the D90 of the heat-affected powder. This suggests that the sieving process can effectively remove powder outside the PSD range of the reference virgin powder. The heat-affected powder PSD indicates that the process-affected powder is substantially larger than the original powder size, which would be effectively removed by sieving. While it is possible that there is process-affect material inside the PSD range of the reference virgin material, their volume and associated accumulation of trace element is insufficient to affect the overall process, as demonstrated by the stable chemical composition throughout the entire recycling program. Thus, it can be concluded that the proposed recycling methodology is effective over the studied range.

reference virgin powder, i.e., the D10 of the oversized powder was higher than the D50 and close to the D90 of the heat-affected powder. This suggests that the sieving process can effectively remove powder outside the PSD range of the reference virgin powder. The heat-affected powder PSD indicates that the process-affected powder is substantially larger than the original powder size, which would be effectively removed by sieving. While it is possible that there is process-affect material inside the PSD range of the reference virgin material, their volume and associated accumulation of trace element is insufficient to affect the overall process, as demonstrated by the stable chemical composition throughout the entire recycling program. Thus, it can be concluded that the proposed recycling methodology is effective over the studied range.

demonstrated by the stable chemical composition throughout the entire recycling program. Thus, it can be concluded that the proposed recycling methodology is effective over the studied range.

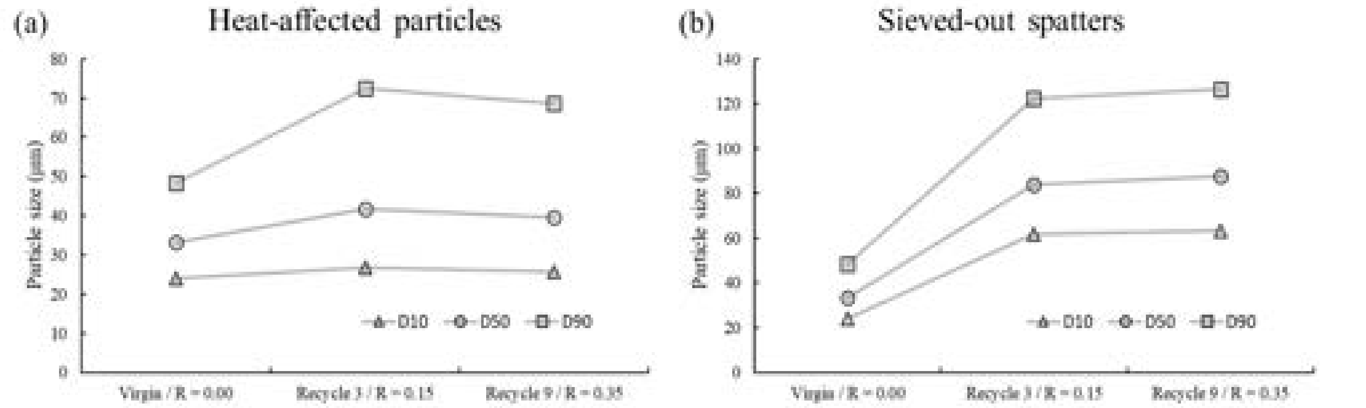

Sustainability **2023**, *15*, x FOR PEER REVIEW 15 of 18

Figure 12. Particle size distribution of (**a**) used powder and (**b**) oversize particles compared to the virgin powder.

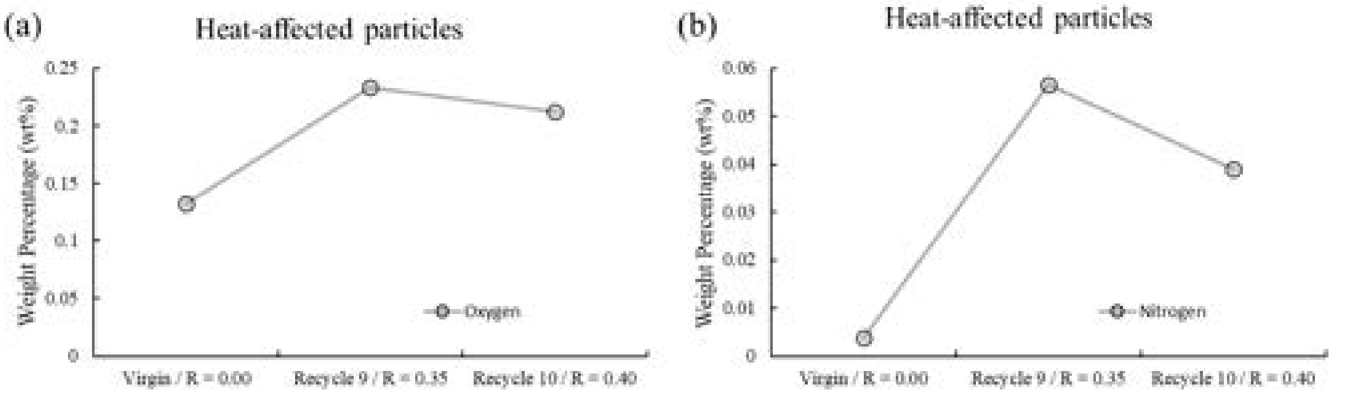

Figure 13. Chemical composition of used powder compared with the virgin powder: (**a**) oxygen content, (**b**) nitrogen content.

4. Conclusions

This work used three recycle metrics (recycle number, BV ratio, and R index) to evaluate the change of powder properties and part properties. The build volume ratio (BV ratio) considers the ratio between consumed powder and input powder, which reflects the effects of laser heating and by-products (e.g., spatters) generated in one build. The R index tracks the total powder consumption and total input powder. This work conducted 10 powder recycles, with BV ratio from 0.12 to 0.22 and R index up to 0.4. The experimental results showed that the powder properties and part tensile properties can be well controlled through recycle methods using sieving and refreshing with virgin powder. The following conclusions can be drawn.

1. Powder particle size showed negligible variation through the 10 recycles. The D_{50} size only changed from 33 μm to 31 μm.
2. Powder compaction and flowability also showed negligible variation through the powder cycles. The Hausner ratio showed a slight stronger correlation with R index, indicating a better compaction in the powder. In general, the changes of Hausner ratio and Hall flow rate are still marginal and have no effect on powder packing and spreading.
3. Oxygen pickup increases with more powder recycles. The powder oxygen content showed stronger linear correlation to the R index (which considers the whole powder usage history) than recycle number and BV ratio. With the fixed processing conditions (chamber oxygen level and laser process parameters), the powder degraded close to the Grade 23 limit after about 40% powder consumption or 10 builds in this work with 0.107% in the virgin powder to 0.129% in the 10th recycled powder.

usage history) than recycle number and BV ratio. With the fixed processing conditions (chamber oxygen level and laser process parameters), the powder degraded close to the Grade 23 limit after about 40% powder consumption or 10 builds in this work with 0.107% in the virgin powder to 0.129% in the 10th recycled powder.

4. The tensile properties showed slight change in yield strength while ultimate strength and ductility (elongation and reduction of area) only fluctuated slightly. The yield strength had the best linear correlation to the BV ratio, then R index and least to recycle number. This implies that the in situ powder degradation (due to thermal exposure and spatters) probably had a more detrimental effect on the yield strength. A possible reason is the potential defects from more spatters generated in a larger printing volume.

In conclusion, powder recycling by sieving and refreshing with virgin powder can effectively control the powder properties except oxygen content. A better powder handling method, including better storage conditions and lower chamber oxygen level, can reduce the powder degradation. Moreover, other powder reprocessing methods (e.g., oxidation reduction) can further reduce material waste. This will be considered in future work to improve the sustainability of LPBF productions.

Author Contributions: Conceptualization: H.S., S.C.V.L. and L.N.S.C.; Funding acquisition: J.Y., C.M. and A.H.; Investigation: T.K., H.S., W.H.K. and M.G.; Methodology: H.S., W.H.K., S.C.V.L. and L.N.S.C.; Project administration: C.M. and A.H.; Supervision: A.H., S.C.V.L. and L.N.S.C.; Writing—original draft: T.K.; Writing—review & editing: H.S., W.H.K., S.C.V.L. and L.N.S.C. All authors have read and agreed to the published version of the manuscript.

Funding: This research was funded by the Shanghai Aircraft Manufacturing Company (ID: 94320).

Institutional Review Board Statement: Not applicable.

Informed Consent Statement: Not applicable.

Data Availability Statement: Data available upon request from the authors.

Acknowledgments: This work is supported by the Shanghai Aircraft Manufacturing Company (ID: 94320). The authors acknowledge the use of facilities within the Monash Centre for Additive Manufacturing (MCAM), as well as the Monash Centre for Electron Microscopy (MCEM), a Node of Microscopy Australia, particularly the electron microscope funded by Australian Research Council grant LE0882821.

Conflicts of Interest: The authors declare no conflict of interest.

References

1. Gibson, I.; Rosen, D.; Stucker, B. *Additive Manufacturing Technologies: 3D Printing, Rapid Prototyping, and Direct Digital Manufacturing*, 2nd ed.; Springer: New York, NY, USA, 2015.
2. Oros Daraban, A.E.; Negrea, C.S.; Artimon, F.G.P.; Angelescu, D.; Popan, G.; Gheorghe, S.I.; Gheorghe, M. A Deep Look at Metal Additive Manufacturing Recycling and Use Tools for Sustainability Performance. *Sustainability* **2019**, *11*, 5494. [CrossRef]
3. Strondl, A.; Lyckfeldt, O.; Brodin, H.; Ackelid, U. Characterization and Control of Powder Properties for Additive Manufacturing. *TMS* **2015**, *67*, 549–554. [CrossRef]
4. Quintana, O.; Alvarez, J.; McMillan, R.; Tong, W.; Tomonto, C. Effects of Reusing Ti-6Al-4V Powder in a Selective Laser Melting Additive System Operated in an Industrial Setting. *TMS* **2018**, *70*, 1863–1869. [CrossRef]
5. Mohd Yusuf, S.; Cutler, S.; Gao, N. Review: The Impact of Metal Additive Manufacturing on the Aerospace Industry. *Metals* **2019**, *9*, 1286. [CrossRef]
6. Khairallah, S.A.; Anderson, A.T.; Rubenchik, A.; King, W.E. Laser powder-bed fusion additive manufacturing: Physics of complex melt flow and formation mechanisms of pores, spatter, and denudation zones. *Acta Mater.* **2016**, *108*, 36–45. [CrossRef]
7. Quinn, P.; O'Halloran, S.; Lawlor, J.; Raghavendra, R. The effect of metal EOS 316L stainless steel additive manufacturing powder recycling on part characteristics and powder reusability. *Adv. Mater. Process. Technol.* **2019**, *5*, 348–359. [CrossRef]
8. Fedina, T.; Sundqvist, J.; Kaplan, A.F.H. Spattering and oxidation phenomena during recycling of low alloy steel powder in Laser Powder Bed Fusion. *Mater. Today Commun.* **2021**, *27*, 102241. [CrossRef]
9. Chu, F.; Zhang, K.; Shen, H.; Liu, M.; Huang, W.; Zhang, X.; Liang, E.; Zhou, Z.; Lei, L.; Hou, J.; et al. Influence of satellite and agglomeration of powder on the processability of AlSi10Mg powder in Laser Powder Bed Fusion. *J. Mater. Res.* **2021**, *11*, 2059–2073. [CrossRef]

10. Bonatti, R.S.; Meyer, Y.A.; Bortolozo, A.D.; Costa, D.; Osório, W.R. Morphology and size effects on densification and mechanical behavior of sintered powders from Al-Si and Al-Cu casting alloys. *J. Alloys Compd.* **2019**, *786*, 717–732. [CrossRef]
11. Satizabal, L.M.; Caurin, H.F.N.; Meyer, Y.A.; Padilha, G.S.; Bortolozo, A.D.; Osório, W.R. Distinct heat treatments and powder size ratios affecting mechanical responses of Al/Si/Cu composites. *J. Compos. Mater.* **2021**, *55*, 3589–3605. [CrossRef]
12. Bonatti, R.S.; Meyer, Y.A.; Padilha, G.S.; Bortolozo, A.D.; Osório, W.R. Silicon Content Affecting Corrosion Behavior of Alp/Sip Composites in a Biodiesel Blend. *Corrosion* **2020**, *76*, 1109–1121. [CrossRef] [PubMed]
13. Nandwana, P.; Peter, W.; Dehoff, R.; Lowe, L.; Kirka, M.; Medina, F.; Babu, S. Recyclability Study on Inconel 718 and Ti-6Al-4V Powders for Use in Electron Beam Melting. *Metall. Mater. Trans. B* **2016**, *47*, 754–762. [CrossRef]
14. Tang, H.; Qian, M.; Liu, N.; Zhang, X.; Yang, G.; Wang, J. Effect of Powder Reuse Times on Additive Manufacturing of Ti-6Al-4V by Selective Electron Beam Melting. *TMS* **2015**, *67*, 555–563. [CrossRef]
15. Popov, V.V.; Katz-Demyanetz, A.; Garkun, A.; Bamberger, M. The effect of powder recycling on the mechanical properties and microstructure of electron beam melted Ti-6Al-4 V specimens. *Addit. Manuf.* **2018**, *22*, 834–843. [CrossRef]
16. Liu, Z.; He, B.; Lyu, T.; Zou, Y. A Review on Additive Manufacturing of Titanium Alloys for Aerospace Applications: Directed Energy Deposition and Beyond Ti-6Al-4V. *JOM* **2021**, *73*, 1804–1818. [CrossRef]
17. Jang, T.-S.; Kim, D.; Han, G.; Yoon, C.-B.; Jung, H.-D. Powder based additive manufacturing for biomedical application of titanium and its alloys: A review. *Biomed. Eng. Lett.* **2020**, *10*, 505–516. [CrossRef]
18. Lütjering, G. *Titanium*, 2nd ed.; Springer: Berlin, UK; New York, NY, USA, 2007.
19. Leicht, A. *Aspects of Building Geometry and Powder Characteristics in Powder Bed Fusion*; Chalmers Tekniska Hogskola: Göteborg, Sweden, 2018.
20. Guoyu, J. The Effect of Oxygen Content on the Tensile Properties of SLMed Ti6Al4V Alloy. Ph.D. Thesis, Monash University, Clayton, VIC, Australia, 2017.
21. Sun, Y.; Aindow, M.; Hebert, R.J. The effect of recycling on the oxygen distribution in Ti-6Al-4V powder for additive manufacturing. *Mater. High Temp Microsc. Oxid.* **2018**, *35*, 217–224. [CrossRef]
22. Silverstein, R.; Eliezer, D. Hydrogen trapping in 3D-printed (additive manufactured) Ti-6Al-4V. *Mater. Charact.* **2018**, *144*, 297–304. [CrossRef]
23. Peterson, J.; Issariyapat, A.; Umeda, J.; Kondoh, K. The effects of heat treatment and carbon content on the microstructure and mechanical properties of laser powder bed fusion Ti-6Al-4V with dissolved TiC particles. *J. Alloys Compd.* **2022**, *920*, 165930. [CrossRef]
24. Liu, L.; Chen, C.; Zhao, R.; Wang, X.; Tao, H.; Shuai, S.; Wang, J.; Liao, H.; Ren, Z. In-situ nitrogen strengthening of selective laser melted Ti6Al4V with superior mechanical performance. *Addit. Manuf.* **2021**, *46*, 102142. [CrossRef]
25. Park, S.B.; Road, B.; Kingdom, U. *Investigating the Effects of Multiple Re-Use of Ti6Al4V Powder in Additive Manufacturing*; Renishaw: Staffordshire, UK, 2016; pp. 1–10.
26. Shalnova, S.A.; Kuzminova, Y.O.; Evlashin, S.A.; Klimova-Korsmik, O.G.; Vildanov, A.M.; Shibalova, A.A.; Turichin, G.A. Effect of recycled powder content on the structure and mechanical properties of Ti-6Al-4V alloy produced by direct energy deposition. *J. Alloys Compd.* **2022**, *893*, 162264. [CrossRef]
27. Yang, K.V.; Looze, G.R.d.; Nguyen, V.; Wilson, R.S. Directed-energy deposition of Ti-6Al-4V alloy using fresh and recycled feedstock powders under reactive atmosphere. *Addit. Manuf.* **2022**, *58*, 103043. [CrossRef]
28. Derimow, N.; Hrabe, N. Oxidation in Reused Powder Bed Fusion Additive Manufacturing Ti-6Al-4V Feedstock: A Brief Review. *JOM* **2021**, *73*, 3618–3638. [CrossRef]
29. Guleryuz, H.; Cimenoglu, H. Oxidation of Ti–6Al–4V alloy. *J. Alloys Compd.* **2009**, *472*, 241–246. [CrossRef]
30. *ASTM E1409-13*; Standard Test Method for Determination of Oxygen and Nitrogen in Titanium and Titanium Alloys by Inert Gas Fusion. ASTM International: West Conshohocken, PA, USA, 2013.
31. *ASTM E1941-10*; Standard Test Method for Determination of Carbon in Refractory and Reactive Metals and Their Alloys by Combustion Analysis. ASTM International: West Conshohocken, PA, USA, 2016.
32. *ASTM E1447-10*; Standard Test Method for Determination of Hydrogen in Titanium and Titanium Alloys by Inert Gas Fusion Thermal Conductivity/Infrared Detection Method. ASTM International: West Conshohocken, PA, USA, 2016.
33. *ASTM E2371-13*; Standard Test Method for Analysis of Titanium and Titanium Alloys by Direct Current Plasma and Inductively Coupled Plasma Atomic Emission Spectrometry (Performance-Based Test Methodology). ASTM International: West Conshohocken, PA, USA, 2013.
34. *ASTM E2651-19*; Standard Guide for Powder Particle Size Analysis. ASTM International: West Conshohocken, PA, USA, 2019.
35. *ASTM B855-17*; Standard Test Method for Volumetric Flow Rate of Metal Powders Using the Arnold Meter and Hall Flowmeter Funnel. ASTM International: West Conshohocken, PA, USA, 2017.
36. *ASTM B964-16*; Standard Test Methods for Flow Rate of Metal Powders Using the Carney Funnel. ASTM International: West Conshohocken, PA, USA, 2016.
37. *ASTM B417-18*; Standard Test Method for Apparent Density of Non-Free-Flowing Metal Powders Using the Carney Funnel. ASTM International: West Conshohocken, PA, USA, 2018.
38. *ASTM B212-21*; Standard Test Method for Apparent Density of Free-Flowing Metal Powders Using the Hall Flowmeter Funnel. ASTM International: West Conshohocken, PA, USA, 2021.

39. Marcu, T.; Todea, M.; Gligor, I.; Berce, P.; Popa, C. Effect of surface conditioning on the flowability of Ti6Al7Nb powder for selective laser melting applications. *Appl. Surf. Sci.* **2012**, *258*, 3276–3282. [CrossRef]
40. Artamonov, V.V.; Bykov, A.O.; Bykov, P.O.; Artamonov, V.P. Measurement of the tap density of metal powders. *Powder Metall. Met. Ceram.* **2013**, *52*, 237–239. [CrossRef]
41. Cao, S.; Chen, Z.; Lim, C.; Yang, K.; Jia, Q.; Jarvis, T.; Tomus, D.; Wu, X. Defect, Microstructure, and Mechanical Property of Ti-6Al-4V Alloy Fabricated by High-Power Selective Laser Melting. *TMS* **2017**, *69*, 2684–2692. [CrossRef]
42. *ASTM E8/E8M*; Standard Test Methods for Tension Testing of Metallic Materials. ASTM International: West Conshohocken, PA, USA, 2016.
43. Alamos, F.J.; Schiltz, J.; Kozlovsky, K.; Attardo, R.; Tomonto, C.; Pelletiers, T.; Schmid, S.R. Effect of powder reuse on mechanical properties of Ti-6Al-4V produced through selective laser melting. *Int. J. Refract. Met. Hard Mater.* **2020**, *91*, 105273. [CrossRef]
44. Suzuki, M.; Sato, H.; Hasegawa, M.; Hirota, M. Effect of size distribution on tapping properties of fine powder. *Powder Technol.* **2001**, *118*, 53–57. [CrossRef]
45. Kaleem, M.A.; Alam, M.Z.; Khan, M.; Jaffery, S.H.I.; Rashid, B. An experimental investigation on accuracy of Hausner Ratio and Carr Index of powders in additive manufacturing processes. *Met. Powder Rep.* **2020**, *76* (Suppl. S1), S50–S54. [CrossRef]
46. Shen, H.; Rometsch, P.; Wu, X.; Huang, A. Influence of Gas Flow Speed on Laser Plume Attenuation and Powder Bed Particle Pickup in Laser Powder Bed Fusion. *JOM* **2020**, *72*, 1039–1051. [CrossRef]
47. Harkin, R.; Wu, H.; Nikam, S.; Quinn, J.; McFadden, S. Reuse of Grade 23 Ti6Al4V Powder during the Laser-Based Powder Bed Fusion Process. *Metals* **2020**, *10*, 1700. [CrossRef]
48. Denti, L.; Sola, A.; Defanti, S.; Sciancalepore, C.; Bondioli, F. Effect of Powder Recycling in Laser-based Powder Bed Fusion of Ti-6Al-4V. *Manuf. Technol.* **2019**, *19*, 190–196. [CrossRef]
49. Carrion, P.; Soltani-Tehrani, A.; Phan, N.; Shamsaei, N. Powder Recycling Effects on the Tensile and Fatigue Behavior of Additively Manufactured Ti-6Al-4V Parts. *JOM* **2019**, *71*, 963–973. [CrossRef]